

## High-pressure ultrasonic study of the Cr–0.3 at. % Ru single-crystal alloy in the commensurate spin-density-wave phase and through the Néel point

M. Cankurtaran,\* G. A. Saunders, H. A. A. Sidek,<sup>†</sup> and Q. Wang  
*School of Physics, University of Bath, Claverton Down, Bath BA2 7AY, United Kingdom*

H. L. Alberts

*Department of Physics, Rand Afrikaans University, P.O. Box 524, Auckland Park 2006, Johannesburg, South Africa*

(Received 23 October 1995)

An experimental ultrasonic study has been made of the elastic and nonlinear acoustic behavior of the antiferromagnetic Cr–0.3 at. % Ru single-crystal alloy in the commensurate (C) spin-density-wave (SDW) phase and then through the Néel point into the paramagnetic phase. The velocities of the ultrasonic modes propagated along the [100] and [110] directions have been measured as a function of hydrostatic pressure up to 0.16 GPa at fixed temperatures in the range from 294 up to 410 K, which covers the Néel point. The results provide complete sets of the elastic-stiffness tensor components and their pressure derivatives as a function of temperature; they lead to an understanding of the interaction between the SDW and the acoustic phonons as the alloy is taken up into the vicinity of the CSDW-to-paramagnetic phase transition. In the CSDW phase all longitudinal and quasilongitudinal modes soften under pressure, implying a strong magnetoelastic interaction between the SDW and long-wavelength longitudinal-acoustic phonons, and in accord with Invar-type behavior of this material. The longitudinal-acoustic-mode Grüneisen parameters have large negative values, the magnitude of which increases as the temperature rises and becomes enormous just below the Néel point; the mode softening is much enhanced. Shear modes tend to stiffen under pressure. The mode gamma  $\gamma_s\{\mathbf{N}[100]\mathbf{U}(001)\}$  of the  $C_{44}$  shear mode has a small positive value and is almost temperature independent throughout the CSDW phase. The mode gamma  $\gamma_s\{\mathbf{N}[110]\mathbf{U}[1\bar{1}0]\}$  pertaining to the  $C'$  shear mode is also small and positive up to 355 K and indicates some softening as the temperature approaches the Néel temperature  $T_{CP}$ . The vibrational anharmonicity of paramagnetic Cr–0.3 at. % Ru is more normal. By contrast to their enormous negative values in the CSDW phase, the longitudinal-acoustic-mode Grüneisen parameters for the alloy in the paramagnetic phase just above the Néel point are positive with values more appropriate for a paramagnetic material; those for shear modes are also positive.

### I. INTRODUCTION

In its antiferromagnetic state below a Néel temperature of 312 K chromium exhibits a transverse spin-density-wave (SDW) structure which is incommensurate with the bcc lattice spacing  $a$ .<sup>1–4</sup> The large amplitude of the static SDW is related to a special geometric feature of the Fermi surface, enabling nesting between the electron and hole pockets, which have similar shapes. These pockets are connected by a nesting vector directed along a [001] axis, nearly, but not quite, equal to the SDW wave vector  $Q$  [ $= (2\pi/a)(1-\delta)$ ] where  $\delta$  is the incommensurability parameter.<sup>2,5–7</sup> Nesting between the electron and hole Fermi surface sheets, which stabilizes the SDW,<sup>8–10</sup> can be improved by dilute alloying with a metallic element (such as Ru, Re, Os or Mn) with more outer electrons to increase the electron to atom ( $e/a$ ) ratio.<sup>4,5,11,12</sup> This raises the Fermi level, thereby increasing the size of the electron Fermi surface while reducing that containing holes. The Néel temperature increases rapidly with introduction of these elements. For an  $e/a$  ratio only slightly larger than the value of six for Cr, the antiferromagnetic SDW periodicity jumps from an incommensurate (I) to a commensurate (C) state.<sup>5,11</sup>

The magnetic phase diagram of many dilute Cr alloys

exhibits a triple point where the paramagnetic (P), the commensurate-SDW (CSDW) and the incommensurate-SDW (ISDW) phases coexist.<sup>4,12</sup> The Cr alloys containing Ru in the region of 1–5 at. % exhibit a CSDW structure below the Néel temperature down to 4 K.<sup>4,13</sup> At lower Ru concentrations the CSDW structure undergoes a transition to the ISDW phase as the temperature is reduced. Hence dilute Cr-Ru alloys can exist in three antiferromagnetic SDW phases:<sup>13,14</sup>

(i) at low temperatures, a longitudinal incommensurate phase existing up to a spin-flip temperature  $T_{SF}$ ,

(ii) above  $T_{SF}$ , a transverse incommensurate phase up to  $T_{IC}$  (the incommensurate-to-commensurate transition temperature),

(iii) above  $T_{IC}$  and below the commensurate-to-paramagnetic Néel temperature ( $T_{CP}$ ), an antiferromagnetic structure commensurate with the lattice (for which the SDW wave vector  $Q$  is equal to  $2\pi/a$ ).

The elastic stiffness of dilute Cr-Ru alloys show well-defined anomalies at  $T_{SF}$ ,  $T_{IC}$ , and  $T_{CP}$ .<sup>4,15–23</sup> The temperature and hydrostatic-pressure dependences of these anomalies observed in monocrystalline Cr–0.3 at. % Ru alloy have been used<sup>18–20</sup> to map (i) the boundary corresponding to the commensurate-to-paramagnetic transition and (ii) the first-

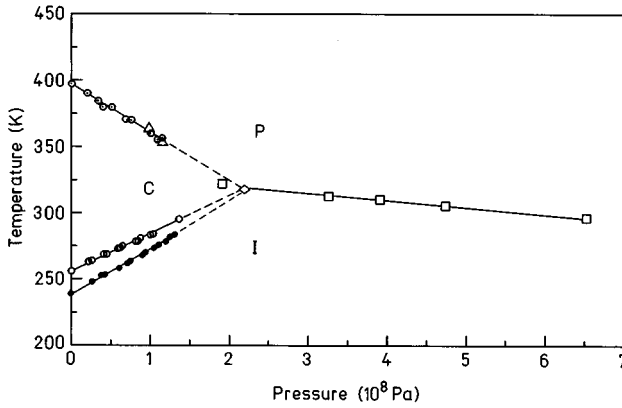


FIG. 1. The pressure-temperature phase diagram of the Cr-0.3 at. % Ru alloy (Ref. 20). The open circles (I-C transition on warming), filled circles (C-I transition on cooling), and encircled dots (C-P transition) were obtained using ultrasonic velocity data (Refs. 19 and 20); the open squares, which refer to the I-P transition, have been taken from Ref. 14. The open triangles on the C-P phase boundary have been obtained from present measurements of the velocities of shear modes propagated along the [100] and [110] directions of the crystal. The estimated triple point, represented by the diamond, is at  $(315 \pm 5)$  K and  $(0.22 \pm 0.02)$  GPa.

order phase boundary between the commensurate and incommensurate spin-density-wave phases on the pressure-temperature phase diagram (Fig. 1). The commensurate-paramagnetic phase boundary is linear with a negative gradient  $dT_{CP}/dP = (-358 \pm 4)$  K/GPa.<sup>20</sup> Both  $T_{CI}$  and  $T_{IC}$  increase approximately linearly with pressure, the mean values of  $dT_{CI}/dP$  and  $dT_{IC}/dP$  being  $(333 \pm 3)$  K/GPa and  $(277 \pm 5)$  K/GPa, respectively.<sup>19,20</sup> The position of the triple point is  $(315 \pm 5)$  K,  $(0.22 \pm 0.02)$  GPa.<sup>19,20</sup>

As a result of the sensitivity of the SDW to the lattice spacing and to the electronic structure and carrier density, the application of pressure can induce large changes in the SDW characteristics of Cr and its dilute alloys. The application of pressure on Cr-0.3 at. % Ru lowers  $T_{CP}$  and increases  $T_{CI}$  (see Fig. 1). This effect is similar to that induced by a decrease in the  $e/a$  ratio, namely, a decrease in the temperature range where the commensurate SDW phase is stable.<sup>4,22</sup> High-pressure ultrasonic studies<sup>18,19</sup> of Cr-0.3 at. % Ru alloy, made in a limited temperature range from 248 to 297 K, have shown that the CSDW phase exhibits particularly instructive nonlinear acoustic behavior. There is a strong magnetoelastic interaction leading to softening of the long-wavelength longitudinal-acoustic phonons under pressure in both the commensurate and incommensurate phases, that in the former phase being much greater and strongly temperature dependent.<sup>19</sup> The acoustic-mode Grüneisen parameters, which quantify the vibrational anharmonicity in the long-wavelength limit, are negative for longitudinal modes in both phases, having much larger magnitudes in the commensurate phase. In the commensurate SDW state both  $(\partial C_{11}/\partial P)_{T,P=0}$  and  $(\partial B^S/\partial P)_{T,P=0}$  are large and negative: a consequence of the longitudinal-mode softening is that the alloy shows the remarkable property that when pressure is applied it becomes easier to squeeze. The aim of the present work has been to extend the measurements of all the elastic-stiffness tensor components over a much wider temperature

range from 294 up to 410 K as a function of hydrostatic pressure in an antiferromagnetic Cr-0.3 at. % Ru single-crystal alloy in the commensurate phase; particular emphasis has been placed on developing an understanding of the interaction between the SDW and the acoustic phonons as the material approaches the vicinity of and then passes through the Néel point into the paramagnetic phase.

## II. EXPERIMENTAL PROCEDURES

The Cr-0.3 at. % Ru single-crystal alloy is the same as that used in previous studies;<sup>18-20</sup> details of the method of growth, its characterization and preparation for ultrasonic experiments are given in Ref. 19. To make the ultrasonic measurements either X- or Y-cut transducers were bonded to the samples using Dow resin. The velocities of 10 MHz ultrasonic waves propagated along the [100] and [110] directions were measured using the pulse-echo-overlap technique.<sup>24</sup> A correction was applied to the ultrasonic wave velocity for multiple reflections at the sample-transducer interface.<sup>25</sup> The measurements at atmospheric pressure of the temperature dependence of ultrasonic wave velocity were made in a thermostatically controlled environment to  $\pm 0.02$  K. The dependence of ultrasonic wave velocity on hydrostatic pressure was measured at fixed temperatures between 294 and 410 K. During pressure runs it was essential to ensure that velocity measurements were made at the same temperature, which was controlled to  $\pm 0.2$  K. Hydrostatic pressure up to about 0.16 GPa was applied using a piston and cylinder apparatus sealed with PTFE and Viton O rings. Silicone fluid was used as the pressure transmitting medium. The pressure was measured using the change in resistance of a precalibrated manganin wire coil (fixed on the sample holder) inside the cell.

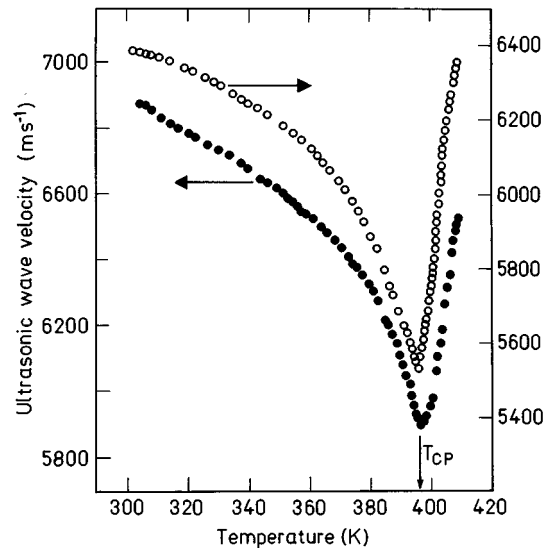


FIG. 2. Temperature dependences of the velocities of longitudinal 10 MHz ultrasonic waves propagated along the [100] ( $C_{11}$  mode: filled circles) and [110] directions ( $C_L$  mode: open circles) in the Cr-0.3 at. % Ru alloy. Points were measured during warming and cooling cycles: there are no hysteresis effects ensuing from passage of the alloy up and down through the Néel temperature  $T_{CP}$ .

To bypass calculation of the changes in crystal dimensions induced by application of hydrostatic pressure, the experimental data was transformed to correspond to the “natural velocity”  $W$ .<sup>26</sup>

### III. TEMPERATURE DEPENDENCES OF THE ELASTIC-STIFFNESS TENSOR COMPONENTS AND BULK MODULUS

The temperature dependences of the velocities of ultrasonic waves propagated along the [100] and [110] directions were measured at atmospheric pressure. These results necessarily comprise an integral component of the subsequent determination of the nonlinear acoustic properties of the Cr–0.3 at. % Ru single-crystal alloy and therefore are presented here (Figs. 2 and 3). Both longitudinal modes along these directions show pronounced mode softening as the temperature is increased; their velocities pass through a sharp and deep minimum at 397 K (Fig. 2), which may be taken<sup>20,23</sup> as that Néel temperature ( $T_{CP}$ ) for transition from the CSDW to the paramagnetic phase. The value determined here for  $T_{CP}$  of Cr–0.3 at. % Ru is in reasonable agreement with the values  $(402 \pm 5)$  K and  $(406 \pm 5)$  K obtained from ultrasonic<sup>16,21</sup> and neutron-diffraction<sup>21</sup> studies, respectively. Measurements made both on warming and cooling through the Néel temperature showed no hysteresis effects: there is no evidence of first-order character. Neutron-diffraction experiments<sup>21</sup> have shown that in Cr–0.3 at. % Ru the CSDW to paramagnetic phase transition is of second order. Similar elastic behavior with temperature in the vicinity of Néel transition has been observed for the longitudinal modes in pure Cr.<sup>27–31</sup>

Measurements of the velocities of all the ultrasonic modes, which can be propagated along the [100] and [110] directions, have been converted into the adiabatic elastic stiffnesses  $C_{11}$ ,  $C_{44}$ ,  $C'$  [ $= (C_{11} - C_{12})/2$ ],  $C_{12}$  and the adiabatic bulk modulus  $B^S$  (Fig. 3). Corrections for the effects of thermal expansion<sup>15</sup> on these elastic moduli have been included but are in fact negligible, being within the experimental error. The agreement between the present results and those of Alberts and Boshoff<sup>16</sup> is reasonable (Fig. 3). Both shear moduli  $C_{44}$  and  $C'$  increase anomalously with increasing temperature towards  $T_{CP}$  where they exhibit a cusp, a behavior similar to that found for pure Cr.<sup>27–31</sup> This stiffening is in complete contrast with the pronounced softening effects of  $C_{11}$ ,  $C_L$ , and the bulk modulus  $B^S$ . As usual the error in  $C_{12}$ , which is obtained from the sums and differences of squared experimental velocity data, is much larger than that for the other elastic-stiffness tensor components; near the Néel temperature  $C_{12}$  becomes very small [see Fig. 3(d)] but the experimental uncertainties are such that it cannot be established if it actually goes slightly negative.

### IV. HYDROSTATIC-PRESSURE DEPENDENCES OF THE ELASTIC-STIFFNESS TENSOR COMPONENTS AND BULK MODULUS

The results of the measurements made at fixed temperatures of the effects of hydrostatic pressure on the velocities of longitudinal and shear waves propagated along the [100]

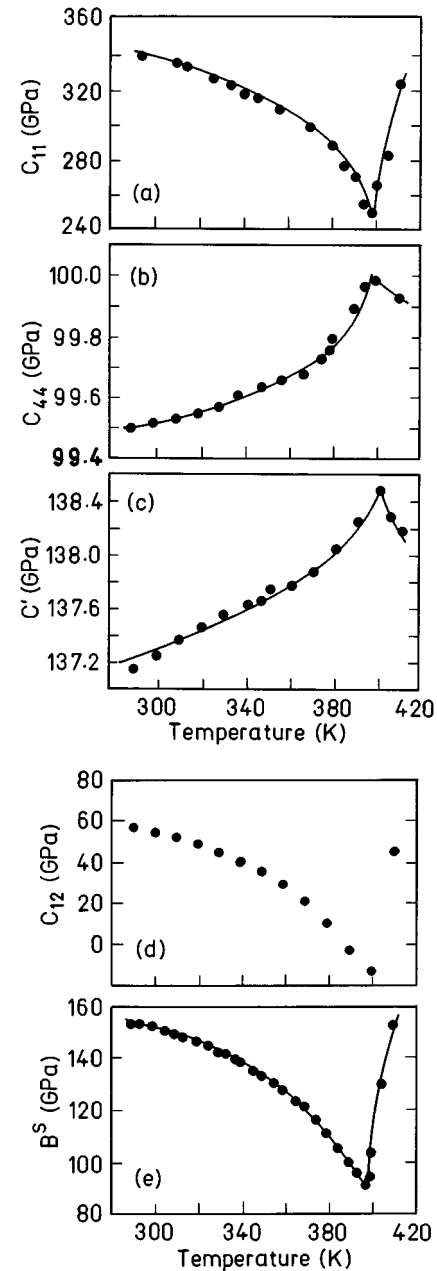


FIG. 3. Temperature dependences of the adiabatic elastic-stiffness tensor components (a)  $C_{11}$ , (b)  $C_{44}$ , (c)  $C' = (C_{11} - C_{12})/2$ , (d)  $C_{12}$ , and (e) the adiabatic bulk modulus  $B^S$  of Cr–0.3 at. % Ru. The solid lines refer to the data of Alberts and Boshoff (Ref. 16).

and [110] directions of Cr–0.3 at. % Ru are presented in Figs. 4–7. In the commensurate phase, well below the Néel transition, the velocities of both longitudinal modes decrease approximately linearly with increasing pressure (Figs. 4 and 5); there is mode softening. The slope of the velocity versus pressure curves increases as temperature is raised: mode softening becomes enhanced. Near the Néel temperature there is a pronounced increase in the gradient at higher pressure (see for example the data given at 326 and 346 K in Fig. 4): this would appear to be a precursor effect of the Néel transition. With a further rise in temperature, the velocity versus pressure curve passes through a deep minimum above which the velocity increases steeply (Figs. 4 and 5): there is mode stiff-

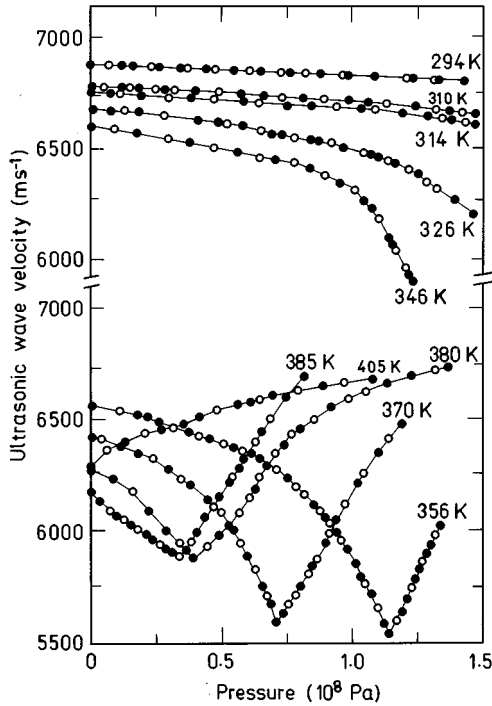


FIG. 4. Hydrostatic-pressure dependence of the velocity of longitudinal 10 MHz ultrasonic waves propagated along the [100] direction in the Cr-0.3 at. % Ru alloy at the temperatures quoted. The filled circles correspond to measurements made with increasing pressure and the open circles to data as the pressure was decreased. There are no hysteresis effects ensuing from passage of the alloy up and down through the Néel point. The lines are for visual guidance.

ening above the minimum. By analogy with the temperature dependence (Fig. 2) the position of the minimum would define the Néel point. The position of the minimum shifts to lower pressure as the temperature is increased; this feature was used<sup>20</sup> to determine the boundary between the CSDW and paramagnetic phases (Fig. 1). The data obtained at 405 K for the  $C_{11}$  mode (Fig. 4) and those at 409 K for the  $C_L$  mode (Fig. 5) correspond to the paramagnetic phase just above  $T_{CP}$ ; they do not define the behavior deep into the paramagnetic phase—the velocity is still a markedly nonlinear function of pressure near  $T_{CP}$ .

Equally interesting behavior is shown by the shear mode velocities when pressure is applied to the Cr-0.3 at. % Ru single-crystal alloy in the commensurate phase (Figs. 6 and 7). At room temperature the velocities of both the  $C'$  [Fig. 6(a)] and  $C_{44}$  [Fig. 7(a)] modes increase slightly as more pressure is applied, the latter more strongly, and then show the effects of the transition from the CSDW to the ISDW phase at about 0.14 GPa, which is characterized by a steep increase in velocity and marked hysteresis due to its first-order nature.<sup>19,21</sup> The effects are much more pronounced for the  $C'$  mode than for the  $C_{44}$  mode. The CSDW to ISDW phase transition was studied in detail by Cankurtaran *et al.*<sup>19</sup> and need not be pursued further here. The nonlinear acoustic behavior of the shear modes in the commensurate phase well below the Néel point can be seen for the  $C'$  mode at 323 K in Fig. 6(b) and for the  $C_{44}$  mode at 322 K in Fig. 7(b): both modes stiffen normally—in contrast to the pronounced softening found for the longitudinal modes (see Figs. 4 and 5).

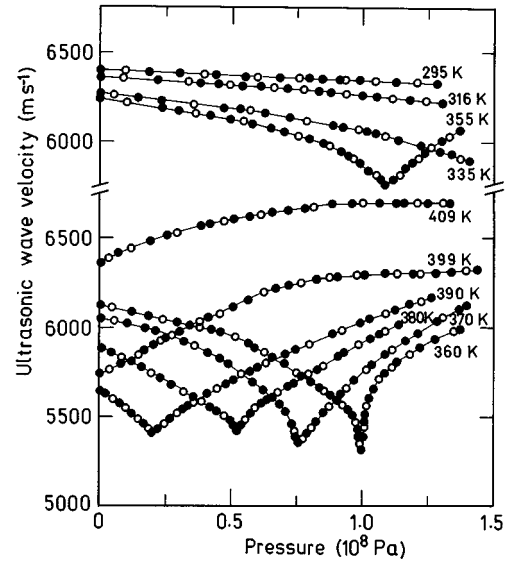


FIG. 5. Hydrostatic-pressure dependence of the velocity of longitudinal 10 MHz ultrasonic waves propagated along the [110] direction in the Cr-0.3 at. % Ru alloy at the temperatures quoted. The filled circles correspond to measurements made with increasing pressure and the open circles to data as the pressure was decreased. There are no hysteresis effects ensuing from passage of the alloy up and down through the Néel point. The lines are for visual guidance.

With a further increase in temperature the onset of the Néel transition to the paramagnetic phase makes an appearance as a large increase in the gradient of the velocity with pressure [Figs. 6(c) and 6(d) and 7(c)–7(e)]. This transition has a finite width: at a still higher pressure its completion can be seen as a knee [see Figs. 6(d) and 6(e) and 7(e)]. The position of the midpoint of the steep rise in velocity in the transition region has been used to provide extra points for the CSDW-paramagnetic boundary on the phase diagram (open triangles in Fig. 1). In the paramagnetic phase (above the knee) both shear modes stiffen normally. Due to softening of the transducer bond, insertion of both ultrasonic shear modes through the crystal became difficult above about 370 K. In the case of the longitudinal modes, magnetic effects on the elastic properties still persist above the Néel point: the velocity versus pressure curves obtained at 405 K for the  $C_{11}$  mode (Fig. 4) and those at 399 and 409 K for the  $C_L$  mode (Fig. 5) show steadily decreasing stiffening as a function of pressure.

The hydrostatic-pressure derivatives  $(\partial C_{IJ}/\partial P)_{T,P=0}$  of the adiabatic second-order elastic-stiffness tensor components  $C_{IJ}$  and  $(\partial B^S/\partial P)_{T,P=0}$  of the adiabatic bulk modulus  $B^S$  for the Cr-0.3 at. % Ru single-crystal alloy, determined from the slope of the pressure dependence of the ultrasonic mode velocity using the formulation described in Ref. 32, are shown as a function of temperature in Fig. 8. In general, in the CSDW phase below about 340 K, the hydrostatic-pressure derivatives  $(\partial C_{11}/\partial P)_{T,P=0}$  and  $(\partial C_L/\partial P)_{T,P=0}$  (corresponding to the longitudinal modes) and also  $(\partial B^S/\partial P)_{T,P=0}$  are negative and much larger in magnitude than those  $(\partial C_{44}/\partial P)_{T,P=0}$  and  $(\partial C'/\partial P)_{T,P=0}$  of shear modes, which are positive. This is a consequence of the

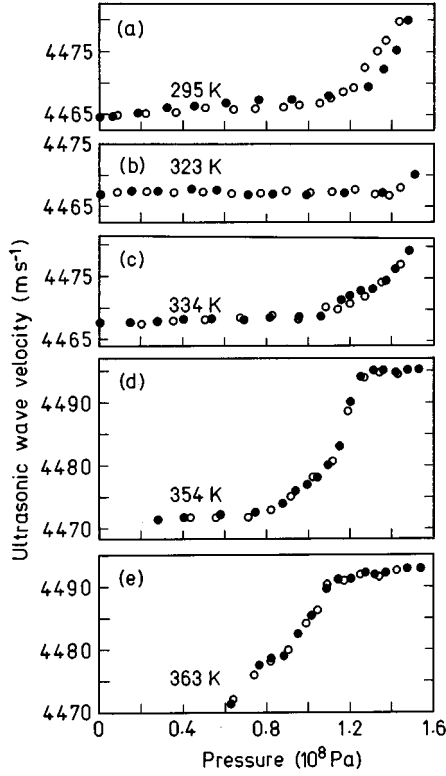


FIG. 6. Hydrostatic-pressure dependence of the velocity of  $[1\bar{1}0]$  polarized shear 10 MHz ultrasonic waves propagated along the  $[110]$  direction in Cr-0.3 at. % Ru at the temperatures quoted. The filled circles correspond to measurements made with increasing pressure and the open circles to data taken as the pressure was decreased.

strong magnetoelastic interaction between the SDW and long-wavelength longitudinal-acoustic phonons, discussed in detail in Ref. 19. With further increase in temperature into the vicinity of the Néel point, the hydrostatic-pressure derivatives  $(\partial C_{11}/\partial P)_{T,P=0}$ ,  $(\partial C_L/\partial P)_{T,P=0}$ , and  $(\partial B^S/\partial P)_{T,P=0}$  become huge negative quantities: the longitudinal-mode softening becomes enormous. Just above the Néel point, another striking effect occurs:  $(\partial C_{11}/\partial P)_{T,P=0}$ ,  $(\partial C_L/\partial P)_{T,P=0}$ , and  $(\partial B^S/\partial P)_{T,P=0}$  become positive quantities. The linear part (above about 0.05 GPa) of the velocity versus pressure curve at 405 K (for the  $C_{11}$  mode) and that at 409 K (for the  $C_L$  mode) has been used to estimate the values of 27.6 and 5.8 for  $(\partial C_{11}/\partial P)_{T,P=0}$  and  $(\partial C_L/\partial P)_{T,P=0}$ , respectively, for Cr-0.3 at. % Ru in the paramagnetic phase.

In the CSDW phase, the hydrostatic-pressure derivatives  $(\partial C_{44}/\partial P)_{T,P=0}$  and  $(\partial C'/\partial P)_{T,P=0}$  of the shear modes are almost independent of temperature (Fig. 8), the former right up to the Néel point. At about 360 K  $(\partial C'/\partial P)_{T,P=0}$  becomes negative and larger in magnitude. Above the Néel point both derivatives become positive. The anharmonicity of the  $C_{44}$  shear mode is only weakly affected by the Néel transition. Using the data points above the knee [Figs. 6(d) and 6(e) and Fig. 7(e)] the values of 3.9 and 2.2 have been deduced for  $(\partial C'/\partial P)_{T,P=0}$  and  $(\partial C_{44}/\partial P)_{T,P=0}$ , respectively, for Cr-0.3 at. % Ru in the paramagnetic phase.

Striking longitudinal-mode softening under pressure has

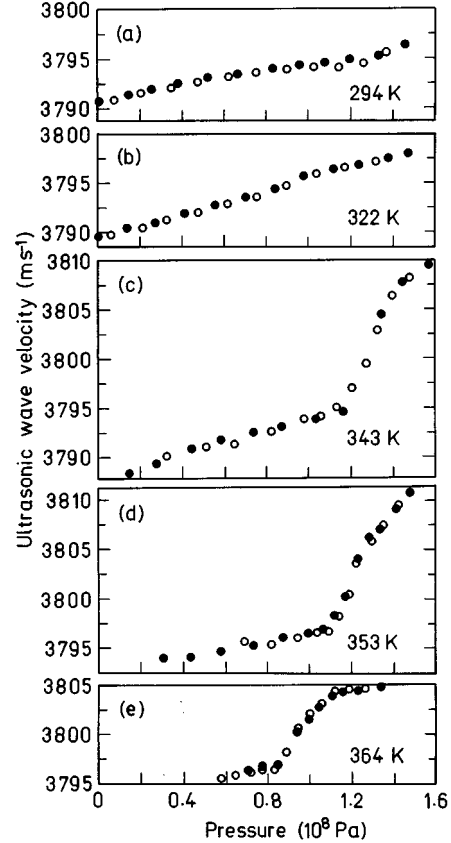


FIG. 7. Hydrostatic-pressure dependence of the velocity of  $(001)$  polarized shear 10 MHz ultrasonic waves propagated along the  $[100]$  direction in Cr-0.3 at. % Ru at the temperatures quoted. The filled circles correspond to measurements made with increasing pressure and the open circles to data taken as the pressure was decreased.

also been observed recently<sup>23</sup> in a Cr-3.5 at. % Al crystal alloy in the CSDW phase. Since the volume of the crystal in the CSDW phase is larger than that in the paramagnetic phase (see Ref. 4), the former state is more sensitive to the effects of applied pressure than the later. The large negative values of  $(\partial C_{11}/\partial P)_{T,P=0}$ ,  $(\partial C_L/\partial P)_{T,P=0}$ , and  $(\partial B^S/\partial P)_{T,P=0}$  found for both the Cr-0.3 at. % Ru and Cr-3.5 at. % Al single-crystal alloys in the CSDW phase show that the material becomes easier to squeeze the more it is pressurized due to the large magnetoelastic interactions.

#### V. ACOUSTIC-MODE GRÜNEISEN PARAMETERS AND VIBRATIONAL ANHARMONICITY OF Cr-0.3 at. % Ru IN THE CSDW AND PARAMAGNETIC PHASES

In the CSDW phase, the large and negative hydrostatic-pressure derivatives of the longitudinal-mode elastic-stiffnesses imply the unusual attribute that under applied pressure the long-wavelength acoustic-mode frequency and energy decrease. Physical insight can be obtained into the considerable changes in the nonlinear acoustic properties which take place as the Cr-0.3 at. % Ru alloy undergoes the transformation from the CSDW to paramagnetic phases by recourse to the mode Grüneisen parameters, which quantify the volume or strain dependence of the lattice vibrational

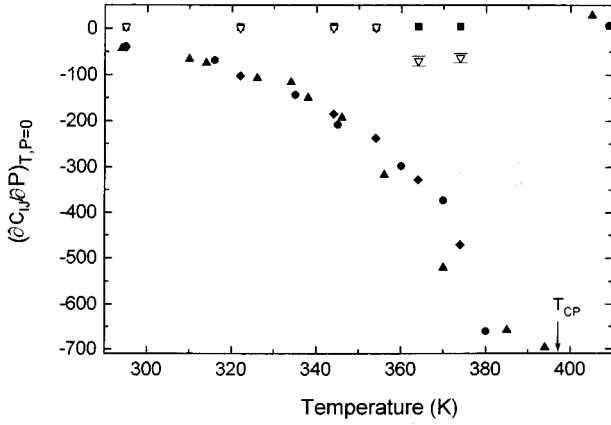


FIG. 8. Temperature dependences of the hydrostatic-pressure derivatives of elastic stiffnesses of Cr-0.3 at. % Ru:  $(\partial C_{11}/\partial P)_{T,P=0}$  (filled triangles),  $(\partial C_L/\partial P)_{T,P=0}$  (filled circles),  $(\partial C_{44}/\partial P)_{T,P=0}$  (filled squares),  $(\partial C'/\partial P)_{T,P=0}$  (open triangles), and  $(\partial B^S/\partial P)_{T,P=0}$  (filled diamonds). The two points at high temperature for  $(\partial C'/\partial P)_{T,P=0}$  marked with error bars have much larger errors, as shown, than the others because they have been obtained indirectly by calculation using data for  $C_{11}$ ,  $C_L$ , and  $C_{44}$  together with their hydrostatic-pressure derivatives.

frequencies in the long-wavelength limit. The dependence of the acoustic-mode frequency  $\omega_p$  in a phonon branch  $p$  on volume ( $V$ ) can be expressed as a mode Grüneisen parameter

$$\gamma_p = - \left( \frac{\partial \ln \omega_p}{\partial \ln V} \right)_T, \quad (1)$$

which can be obtained from measurements of the elastic-stiffness tensor components (Fig. 3) and their dependences on hydrostatic pressure (Fig. 8). Hence it is possible to determine and compare the acoustic-mode Grüneisen parameters in the CSDW and paramagnetic phases and find out the degree to which the magnetoelastic interactions influence the vibrational anharmonicity of the acoustic phonons. To enable the required comparison, the acoustic-mode Grüneisen parameters have been calculated as a function of propagation direction, using the method developed by Brugger and Fritz,<sup>33</sup> for the CSDW phase at 294, 354, and 374 K (Fig. 9) and for the paramagnetic phase just above the Néel point [Fig. 10(a)]. In the CSDW phase, at 294 K, a temperature well below  $T_{CP}$  at which the Néel transition takes place at atmospheric pressure, the most striking feature is that the longitudinal-mode Grüneisen parameters have large negative values, while those of the shear modes have more normal, small positive values. These general characteristics, previously found<sup>19</sup> at lower temperatures in the CSDW phase of Cr-0.3 at. % Ru and also more recently for Cr-3.5 at. % Al in the CSDW phase,<sup>23</sup> established the existence of a strong interaction between the zone-center longitudinal acoustic phonons and the SDW. The finding that the mode gammas in a given branch do not vary much with propagation direction shows that the SDW interacts strongly with all the longitudinal- and quasilongitudinal-acoustic modes in the long-wavelength limit to about the same extent; the interaction is effectively isotropic. At temperatures well below the

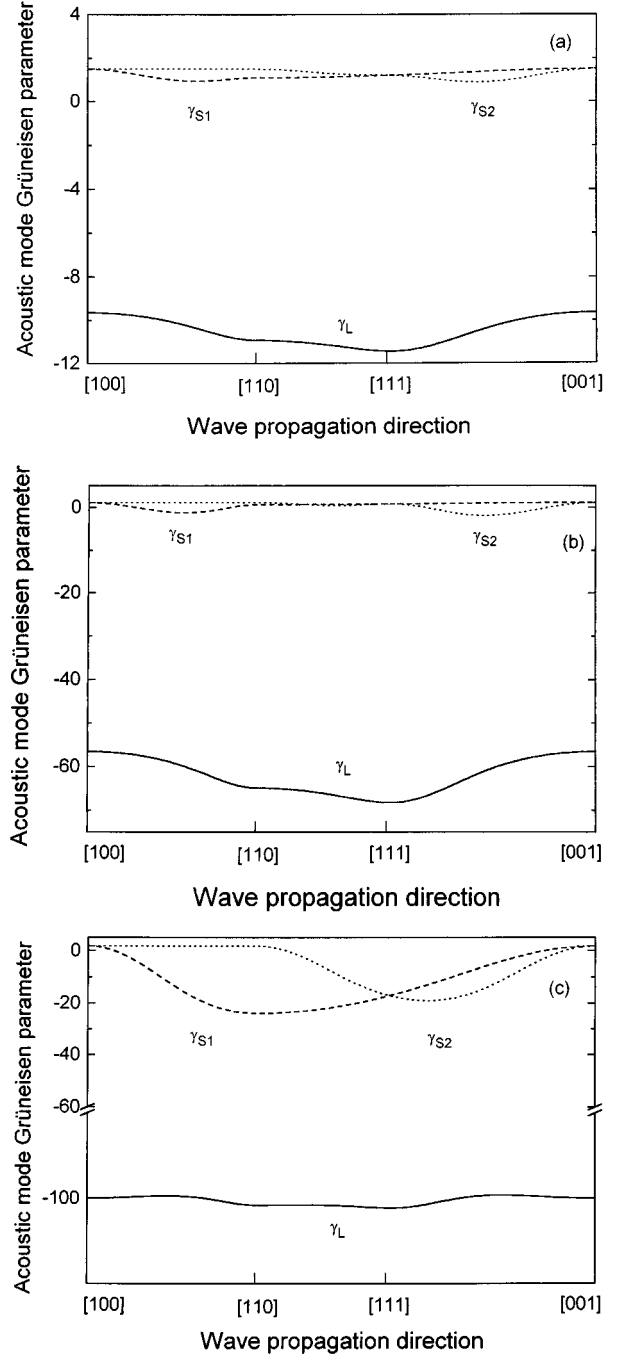


FIG. 9. Long-wavelength longitudinal (solid line) and shear (dashed and dotted lines) acoustic-mode Grüneisen parameters as a function of mode propagation direction for Cr-0.3 at. % Ru in the CSDW phase at (a) 294 K, (b) 354 K, and (c) 374 K.

Néel transition the shear-mode Grüneisen parameters are small—in accord with previous observations for Cr-0.3 at. % Ru (Ref. 19) and for Cr-3.5 at. % Al (Ref. 23). The order of magnitude difference between the longitudinal and shear-mode Grüneisen parameters, led to the conclusion that strong magnetoelastic coupling in the CSDW phase takes place mainly through volume strain, although there are also contributions from the shear strains.

Consideration of the evolution of vibrational anharmonicity in the CSDW phase as the temperature is raised towards

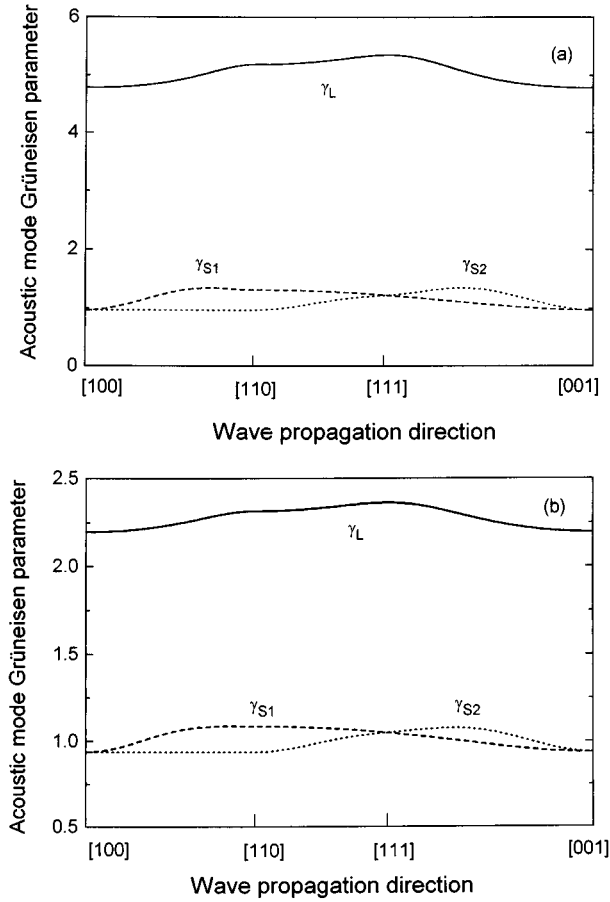


FIG. 10. Long-wavelength longitudinal (solid line) and shear (dashed and dotted lines) acoustic-mode Grüneisen parameters as a function of mode propagation direction (a) for the Cr-0.3 at. % Ru alloy in the paramagnetic phase just above the Néel point, and (b) for a Cr-5 at. % V alloy (at 295 K), which remains paramagnetic at all temperatures (taken from Ref. 34).

$T_{CP}$  exposes further interesting features of the magnetoelastic interactions. The plots of the acoustic-mode Grüneisen parameters as a function of propagation direction at 354 K [Fig. 9(b)] and 374 K [Fig. 9(c)] show that, while remaining essentially isotropic, the longitudinal-mode gammas increase rapidly to enormously large negative quantities as the temperature rises; the mode softening, which is such a characteristic feature of the CSDW phase, becomes greatly enhanced. Furthermore anomalous behavior of the shear-mode gammas becomes apparent, especially for  $\gamma_s\{\mathbf{N}[110]\mathbf{U}[1\bar{1}0]\}$  corresponding to the  $C'$  mode (i.e., propagation vector  $\mathbf{N}$  along the twofold [110] direction and polarization vector along another twofold  $[1\bar{1}0]$  direction). At 354 K, the shear-mode gammas are slightly negative in certain directions. However, at 374 K (much closer to  $T_{CP}$ )  $\gamma_s\{\mathbf{N}[110]\mathbf{U}[1\bar{1}0]\}$  has the large negative value of about -23: this mode is also softening. The mode gamma  $\gamma_s\{\mathbf{N}[100]\mathbf{U}(001)\}$ , corresponding to the  $C_{44}$  mode [i.e., propagation vector  $\mathbf{N}$  along the fourfold [100] direction and polarization vector  $\mathbf{U}$  in the (001) plane], retains a small positive value. Many of the quasishear modes, which propa-

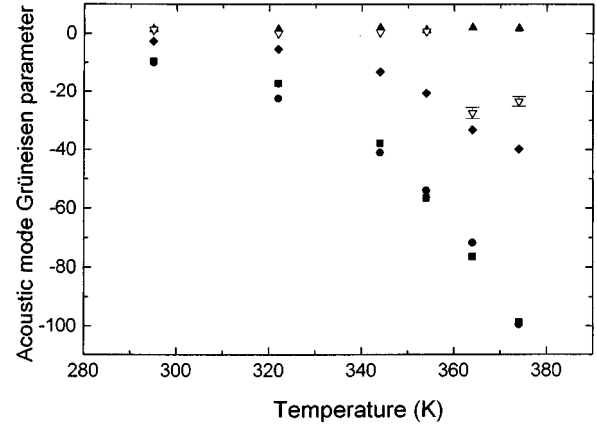


FIG. 11. Temperature dependences of the long-wavelength acoustic-mode Grüneisen parameters of Cr-0.3 at. % Ru in the CSDW phase. Longitudinal modes:  $\gamma_{11}[100]$  (filled squares) and  $\gamma_L[110]$  (filled circles); shear modes:  $\gamma_s\{\mathbf{N}[100]\mathbf{U}(001)\}$  [i.e., propagation vector  $\mathbf{N}$  along the fourfold [100] direction and polarization vector  $\mathbf{U}$  in the (001) plane] (filled triangles) and  $\gamma_s\{\mathbf{N}[110]\mathbf{U}[1\bar{1}0]\}$  (open triangles). The two points at high temperature for  $\gamma_s\{\mathbf{N}[110]\mathbf{U}[1\bar{1}0]\}$  marked with error bars have much larger errors, as shown, than the others because they have been obtained indirectly by calculation using data for  $C_{11}$ ,  $C_L$ , and  $C_{44}$  together with their hydrostatic-pressure derivatives. The mean acoustic-mode Grüneisen parameter  $\gamma^{el}$  is denoted by the filled diamonds.

gate along nonsymmetry directions, also show a tendency to soften as the temperature approaches  $T_{CP}$  [see Fig. 9(b)].

The temperature dependences of the Grüneisen parameters for the pure acoustic modes of Cr-0.3 at. % Ru in the CSDW phase are shown in Fig. 11. As the temperature approaches  $T_{CP}$ , the longitudinal-mode gammas,  $\gamma_{11}[100]$  and  $\gamma_L[110]$ , become extremely large: the mode softening induced by the magnetoelastic interaction with the SDW is much enhanced. The Grüneisen gamma  $\gamma_s\{\mathbf{N}[100]\mathbf{U}(001)\}$  corresponding to the  $C_{44}$  mode remains essentially constant throughout the whole temperature range (from 250 to 365 K) of the existence of the CSDW phase: the weak interaction of the SDW with this pure shear mode does not change appreciably with temperature. The Grüneisen gamma  $\gamma_s\{\mathbf{N}[110]\mathbf{U}[1\bar{1}0]\}$  corresponding to the  $C'$  mode also stays constant up to about 355 K. Above this temperature  $\gamma_s\{\mathbf{N}[110]\mathbf{U}[1\bar{1}0]\}$  takes on a negative sign and increases in magnitude: there is also softening of the  $C'$  mode as temperature is raised towards  $T_{CP}$ . It should be remarked that a reduction of  $C_{11}$  (see Fig. 2) can be instrumental in reducing  $C'$  [=  $(C_{11} - C_{12})/2$ ] in turn; similarly an increase of the magnitude of  $(\partial C_{11}/\partial P)_{T,P=0}$  can result in increase in magnitude of  $(\partial C'/\partial P)_{T,P=0}$ : such linkage implies that a mechanism which softens  $C_{11}$  can be reflected in the behavior of  $C'$  and of  $(\partial C'/\partial P)_{T,P=0}$  with temperature and this could be the case here. Figure 11 clearly illustrates the dominating role of the interaction between the SDW and the long-wavelength longitudinal-acoustic phonons in the nonlinear acoustic behavior of Cr-0.3 at. % Ru in the CSDW phase and near the Néel transition. Similar results were also

found<sup>23</sup> for Cr-3.5 at. % Al. The magnetoelastic coupling effects in the CSDW phase of these two alloys are significantly larger for the volume-dependent longitudinal modes than for the volume-conserving shear modes.

The mean long-wavelength acoustic Grüneisen parameter  $\gamma^{\text{el}}$ , which is a measure of the overall contribution of zone-center acoustic modes to the lattice vibrational anharmonicity, can be calculated by summing all of the long-wavelength acoustic-mode Grüneisen parameters with the same weight for each mode using

$$\gamma^{\text{el}} = \frac{\sum_{p=1}^3 \int_{\Omega} \gamma_p d\Omega}{3 \int_{\Omega} d\Omega}. \quad (2)$$

Here the integration is over the whole space  $\Omega$ .  $\gamma^{\text{el}}$  of Cr-0.3 at. % Ru is negative in the CSDW phase; its magnitude increases strongly as the Néel point is approached (see Fig. 11), above which it jumps to a positive value of (2.45)—larger than that (1.45) found<sup>34</sup> for  $\gamma^{\text{el}}$  of paramagnetic Cr-5 at. % V. A negative  $\gamma^{\text{el}}$  has also been reported<sup>23</sup> for Cr-3.5 at. % Al in the CSDW phase, which is smaller in magnitude than that for Cr-0.3 at. % Ru and remains nearly temperature independent.

Now we can turn to discuss the vibrational anharmonicity of the Cr-0.3 at. % Ru alloy in the paramagnetic phase. The acoustic-mode Grüneisen parameters of Cr-0.3 at. % Ru in the paramagnetic phase just above the Néel point are plotted in Fig. 10(a) as a function of propagation direction. Both longitudinal and shear-mode gammas are positive. By complete contrast to the huge and negative values in the CSDW phase, the longitudinal mode gammas are positive and have values appropriate for a paramagnetic material. A useful way to assess the physical significance of these acoustic-mode Grüneisen parameters in the paramagnetic phase is to compare them with those determined<sup>34</sup> for a Cr-5 at. % V single-crystal alloy. Since Cr-V alloys containing greater than 4 at. % V remain paramagnetic at all temperatures (see the phase diagram in Fig. 11 of Ref. 4), the Cr-5 at. % V alloy has often been used as a reference material to define the nonmagnetic behavior of Cr and its alloys (for a recent review see Ref. 4). Addition of V to Cr reduces the electron concentration, and suppresses the magnetic transition so that alloying Cr with V does not change the lattice dynamics or phonon-dispersion relations significantly. Inspection of Fig. 10 shows that shear-mode Grüneisen parameters of paramagnetic Cr-0.3 at. % Ru alloy are almost the same as those of Cr-5 at. % V. However, although now positive, the longitudinal-mode Grüneisen gammas of paramagnetic Cr-0.3 at. % Ru are about twice as large as those of Cr-5 at. % V, indicating that some effects of magnetic ordering on the longitudinal modes are retained in the Cr-0.3 at. % Ru above the Néel transition.

Any theoretical consideration of magnetoelasticity in this SDW system should be able to account for the large magnetoelastic interactions of the SDW in particular with longitudinal-acoustic phonons.

The anomalies observed in the temperature dependence of magnetoelastic properties of Cr and antiferromagnetic Cr alloys have been commonly described in terms of magnetic Grüneisen parameters, which are taken as a measure of the

strength of the magnetoelastic coupling (for a review see Ref. 4). The magnetic Grüneisen parameter  $\Gamma_{\text{CP}}$  can be obtained directly from the hydrostatic-pressure dependence of  $T_{\text{CP}}$  using

$$\Gamma_{\text{CP}} = \frac{B_{\text{CP}}}{T_{\text{CP}}} \frac{dT_{\text{CP}}}{dP}, \quad (3)$$

where  $B_{\text{CP}}$  is the bulk modulus at  $T_{\text{CP}}$  at atmospheric pressure. From the present data a value of  $(-81 \pm 3)$  has been obtained for  $\Gamma_{\text{CP}}$  of Cr-0.3 at. % Ru, which is close to that  $(-80)$  given in Ref. 4. The large value of  $\Gamma_{\text{CP}}$  at the CSDW-to-paramagnetic transition implies that the magnetoelastic coupling, associated with the mechanisms responsible for destruction of magnetic order with increasing temperature through the Néel point, is very strong. To derive Eq. (3) it is assumed that the magnetic contribution to the free energy is separable and is a function of a single, volume-dependent temperature parameter (see for instance Refs. 4 and 35–37). In practice it is not possible to separate the magnetic contributions from the electronic or lattice contributions to the free energy.<sup>4,38,39</sup> In fact the results of the present measurements show that not only the volume strain but also shear strains (although to a much lesser extent) are involved in the CSDW-to-paramagnetic transition. Nevertheless, it is instructive to compare the huge value of the magnetic Grüneisen parameter  $\Gamma_{\text{CP}}$  with the similarly large longitudinal-acoustic-mode Grüneisen parameters  $\gamma_{11}[100]$  and  $\gamma_L[110]$  in the CSDW phase below the Néel point (see Fig. 11). The fact that the value of  $\Gamma_{\text{CP}}$  is comparable with those of  $\gamma_{11}[100]$  and  $\gamma_L[110]$  just below the Néel transition, provides support for the use of the thermodynamic model,<sup>4,35</sup> which leads to Eq. (3), to analyze the data for the magnetoelasticity of Cr-0.3 at. % Ru in the CSDW phase in the vicinity of the Néel point.

## VI. CONGRUENCE BETWEEN ACOUSTIC-MODE SOFTENING IN Cr-0.3 at. % Ru AND INVAR ALLOYS

In the CSDW phase of the Cr-0.3 at. % Ru alloy, below the Néel transition, it has been found that the velocities of both longitudinal modes decrease almost linearly with increasing pressure: there is mode softening under pressure, which becomes enhanced at higher temperatures. Pronounced softening effects are found for longitudinal elastic stiffnesses  $C_{11}$  and  $C_L$  and also for the bulk modulus  $B^S$  as the temperature is increased at atmospheric pressure; they pass through a deep minimum at the Néel temperature ( $T_{\text{CP}}$ ) for transition from the CSDW to the paramagnetic phase. Soft longitudinal-acoustic modes are known to play an important role in the Invar behavior of ferromagnetic iron alloys.<sup>40–43</sup> Mañosa *et al.*<sup>40</sup> found experimental evidence for longitudinal-acoustic-mode softening in ferromagnetic  $\text{Fe}_{72}\text{Pt}_{28}$  and argued that this behavior is central to understanding the source of the negative thermal expansion of this Invar alloy. The pressure derivatives  $(\partial C_{11}/\partial P)_{T,P=0}$  and  $(\partial C_L/\partial P)_{T,P=0}$ , of the longitudinal-mode elastic stiffnesses and that  $(\partial B^S/\partial P)_{T,P=0}$  of the adiabatic bulk modulus are negative in the ferromagnetic phase of  $\text{Fe}_{72}\text{Pt}_{28}$ , while being positive in the paramagnetic phase. Hence the Grüneisen parameters of the volume-dependent longitudinal-

acoustic modes are strongly negative in the Invar region, accounting for the negative thermal expansion observed<sup>44</sup> in ferromagnetic Fe<sub>72</sub>Pt<sub>28</sub> in the temperature range between about 260 K and the Curie temperature. Thus the anomalous vibrational anharmonicity of long-wavelength longitudinal-acoustic modes, which is due to the strong magnetoelastic interactions, is largely responsible for the Invar behavior of Fe<sub>72</sub>Pt<sub>28</sub>. The present measurements reveal that the same kind of longitudinal-mode softening occurs in Cr-0.3 at. % Ru in the CSDW phase. This fact, together with an earlier observation<sup>15</sup> that the coefficient of thermal expansion is zero near the Néel temperature, strongly suggest that Cr-0.3 at. % Ru show antiferromagnetic Invar-type behavior and that magnetoelastic interactions lead to the longitudinal mode softening in the CSDW phase of antiferromagnetic Cr-0.3 at. % Ru. Above the Néel temperature the magnetoelastic interaction diminishes sharply and the usual positive contribution from vibrational anharmonicity becomes dominant, giving positive acoustic-mode Grüneisen parameters. These observations are similar in kind to the effects found in ferromagnetic Fe<sub>72</sub>Pt<sub>28</sub> Invar alloy as it goes through the Curie temperature, including change in sign of  $\gamma^{\text{el}}$ .<sup>40</sup> An explanation for the anomalous temperature dependences of the adiabatic bulk modulus  $B^S$  and its hydrostatic pressure derivative  $(\partial B^S/\partial P)_{T,P=0}$  for Fe<sub>72</sub>Pt<sub>28</sub>, which show pronounced minima in the Invar region, was shown<sup>42</sup> to be entirely consistent with the recently developed theories of Invar alloys.<sup>39,45,46</sup> Acoustic-mode softening is also found in R<sub>2</sub>Fe<sub>12</sub>B-type compounds (R=Y,Nd,Er), which exhibit Invar properties. From elastic constant measurements by using an ultrasonic pulse echo technique Shiga and Nakamura<sup>47</sup> determined the temperature dependence of the bulk modulus of Y<sub>2</sub>Fe<sub>12</sub>B near the Curie temperature at zero applied magnetic field. They found a typical  $\lambda$ -type dip, indicating a critical softening due to the second-order phase transition. Similar results were also obtained by Shiga *et al.*<sup>48</sup> for Nd<sub>2</sub>Fe<sub>12</sub>B. Sidorov and Khvostantsev<sup>49</sup> used a strain-gauge technique to study the behavior of the bulk modulus of Er<sub>2</sub>Fe<sub>12</sub>B near the Curie point as a function of hydrostatic pressure. The pressure dependence of the bulk modulus of Er<sub>2</sub>Fe<sub>12</sub>B showed a pronounced  $\lambda$ -type anomaly due to the ferromagnetic-to-paramagnetic transition at the Curie point. Since no hysteresis effects were found in the pressure dependence of the relative volume change, the giant softening of the bulk modulus of the Er<sub>2</sub>Fe<sub>12</sub>B Invar system under pressure was attributed to the strong magnetoelastic interactions at the second-order magnetic transition. Acoustic-mode softening due to magnetoelastic interactions is a common feature of these Invar materials.

## VII. CONCLUSIONS

The velocities of the ultrasonic modes propagated in the [100] and [110] directions of antiferromagnetic Cr-0.3 at. % Ru single-crystal alloy in the commensurate phase have been measured as a function of hydrostatic pressure up to 0.16 GPa at fixed temperatures in the range from 294 to 410 K, which covers the Néel point. The results have led to an understanding of the interaction between the SDW and the acoustic phonons as this alloy is taken up into the vicinity

and then through the Néel point into the paramagnetic phase. The physical significance of the results can be summarized as follows:

(i) Pronounced softening effects are found for longitudinal elastic stiffnesses  $C_{11}$  and  $C_L$  and also for the bulk modulus  $B^S$  as the temperature is increased at atmospheric pressure; they pass through a deep minimum at 397 K, which may be taken as the Néel temperature ( $T_{\text{CP}}$ ) for transition from the CSDW to the paramagnetic phase. By contrast, the shear moduli  $C_{44}$  and  $C'$  increase anomalously with increasing temperature towards  $T_{\text{CP}}$  where they exhibit a cusp. No hysteresis effects have been observed.

(ii) In the CSDW phase, well below the Néel transition, the velocities of both longitudinal modes decrease almost linearly with increasing pressure: there is mode softening under pressure, which becomes enhanced at higher temperatures. With a further rise in temperature, the velocity versus pressure curve passes through a deep minimum above which the velocity increases steeply (there is mode stiffening above the minimum). The position of the minimum shifts to lower pressure as the temperature is increased. In the CSDW phase the velocities of both shear modes stiffen normally. Steplike changes in the gradient mark the onset and completion of the CSDW-to-paramagnetic phase transition. In the paramagnetic phase the gradient of the velocity versus pressure curve is positive and has a value in a more normal range of shear modes.

(iii) Magnetic effects in the elastic and nonlinear acoustic properties of longitudinal modes persist somewhat above the Néel point.

(iv) In the CSDW phase the hydrostatic-pressure derivatives  $(\partial C_{11}/\partial P)_{T,P=0}$  and  $(\partial C_L/\partial P)_{T,P=0}$  and also  $(\partial B^S/\partial P)_{T,P=0}$  are negative and have a larger magnitude, implying a strong magnetoelastic interaction between the SDW and long-wavelength longitudinal-acoustic phonons. Just below the Néel point,  $(\partial C_{11}/\partial P)_{T,P=0}$ ,  $(\partial C_L/\partial P)_{T,P=0}$ , and  $(\partial B^S/\partial P)_{T,P=0}$  become huge negative quantities: the longitudinal-mode softening becomes enormous.

(v) In the paramagnetic phase just above the Néel point  $(\partial C_{11}/\partial P)_{T,P=0}$  and  $(\partial C_L/\partial P)_{T,P=0}$  are positive: there is no longitudinal-acoustic-mode softening.

(vi) In the CSDW phase at temperatures well below  $T_{\text{CP}}$ , the longitudinal-acoustic-mode Grüneisen parameters have large negative values, while those of the shear modes have more normal, small positive values. This evidences a strong interaction between the zone-center longitudinal-acoustic phonons and the SDW. While remaining essentially isotropic, the longitudinal-mode gammas increase enormously to large negative quantities as the temperature rises towards  $T_{\text{CP}}$ ; the mode softening induced by the magnetoelastic interaction with the SDW is much enhanced.

(vii) In the CSDW phase  $(\partial C_{44}/\partial P)_{T,P=0}$  has an almost temperature independent, small, positive value, and takes about the same value in the paramagnetic phase. While  $(\partial C'/\partial P)_{T,P=0}$  has a similar value below about 355 K, it becomes negative and larger in magnitude near the Néel point. In the paramagnetic phase  $(\partial C'/\partial P)_{T,P=0}$  takes a value which is reasonable for a paramagnetic crystal. The

mode gamma  $\gamma_s\{\mathbf{N}[100]\mathbf{U}(001)\}$  corresponding to the  $C_{44}$  mode has a small positive value and is almost temperature independent throughout the CSDW phase. The shear-mode gamma  $\gamma_s\{\mathbf{N}[110]\mathbf{U}[1\bar{1}0]\}$  evidences softening of the  $C'$  mode as the temperature approaches  $T_{CP}$ .

(viii) The Invar-like behavior of antiferromagnetic Cr-0.3 at. % Ru single-crystal alloy in the commensurate phase is characteristically associated with the longitudinal-acoustic-mode softening.

## ACKNOWLEDGMENTS

We are grateful to our colleagues R. C. J. Draper, E. F. Lambson, and W. A. Lambson for technical assistance. H. A. A. Sidek is grateful to the Universiti Pertanian Malaysia and to the Public Service Department of Malaysia for granting study leave and for the financial support provided through the ADB-Industrial Development Programme. H. L. Alberts would like to thank the South African FRD for financial support.

- \*Permanent address: Hacettepe University, Department of Physics, Beytepe, 06532 Ankara, Turkey.
- †Permanent address: Department of Physics, Universiti Pertanian, 43400 Serdang Selangor, Malaysia.
- <sup>1</sup>A. W. Overhauser, *Phys. Rev.* **128**, 1437 (1962).
- <sup>2</sup>S. A. Werner, A. Arrott, and H. Kendrick, *Phys. Rev.* **155**, 528 (1967).
- <sup>3</sup>E. Fawcett, *Rev. Mod. Phys.* **60**, 209 (1988).
- <sup>4</sup>E. Fawcett, H. L. Alberts, V. Yu. Galkin, D. R. Noakes, and J. V. Yakhmi, *Rev. Mod. Phys.* **66**, 25 (1994).
- <sup>5</sup>W. C. Koehler, R. M. Moon, A. L. Trego, and A. R. Mackintosh, *Phys. Rev.* **151**, 405 (1966).
- <sup>6</sup>H. Umebayashi, G. Shirane, B. C. Frazer, and W. B. Daniels, *J. Phys. Soc. Jpn.* **24**, 368 (1968).
- <sup>7</sup>W. J. Venema, R. Griessen, and W. Ruesink, *J. Phys. F* **10**, 2841 (1980).
- <sup>8</sup>W. M. Lomer, *Proc. Phys. Soc. London* **80**, 489 (1962).
- <sup>9</sup>J. Rath and J. Callaway, *Phys. Rev. B* **8**, 5398 (1973).
- <sup>10</sup>D. G. Laurent, J. Callaway, J. L. Fry, and N. E. Brener, *Phys. Rev. B* **23**, 4977 (1981).
- <sup>11</sup>L. M. Falicov and D. R. Penn, *Phys. Rev.* **158**, 476 (1967).
- <sup>12</sup>N. I. Kulikov and V. V. Tugushev, *Sov. Phys. Usp.* **27**, 954 (1984).
- <sup>13</sup>R. Papoular, D. Debray, and S. Araj, *J. Magn. Magn. Mater.* **24**, 106 (1981).
- <sup>14</sup>A. Jayaraman, T. M. Rice, and E. Bucher, *J. Appl. Phys.* **41**, 869 (1970).
- <sup>15</sup>H. L. Alberts and J. A. J. Lourens, *J. Phys. F* **18**, L213 (1988).
- <sup>16</sup>H. L. Alberts and A. H. Boshoff, *J. Magn. Magn. Mater.* **104-107**, 2031 (1992).
- <sup>17</sup>E. Fawcett and H. L. Alberts, *J. Phys. Condens. Matter* **4**, 613 (1992).
- <sup>18</sup>H. L. Alberts, P. J. Ford, H. Rahdi, and G. A. Saunders, *J. Phys. Condens. Matter* **4**, 2793 (1992).
- <sup>19</sup>M. Cankurtaran, G. A. Saunders, Q. Wang, P. J. Ford, and H. L. Alberts, *Phys. Rev. B* **46**, 14 370 (1992).
- <sup>20</sup>H. A. A. Sidek, M. Cankurtaran, G. A. Saunders, P. J. Ford, and H. L. Alberts, *Phys. Lett. A* **172**, 387 (1993).
- <sup>21</sup>A. H. Boshoff, H. L. Alberts, P. de V. du Plessis, and A. M. Venter, *J. Phys. Condens. Matter* **5**, 5353 (1993).
- <sup>22</sup>P. P. Mokheseng, H. L. Alberts, and P. Smit, *J. Phys. Condens. Matter* **6**, L337 (1995).
- <sup>23</sup>H. L. Alberts and P. Smit, *Phys. Rev. B* **51**, 15 146 (1995).
- <sup>24</sup>E. P. Papadakis, *J. Acoust. Soc. Am.* **42**, 1045 (1967).
- <sup>25</sup>E. Kittinger, *Ultrasonics* **15**, 30 (1977).
- <sup>26</sup>R. N. Thurston and K. Brugger, *Phys. Rev.* **133**, A1604 (1964).
- <sup>27</sup>D. I. Bolef and J. de Klerk, *Phys. Rev.* **129**, 1063 (1963).
- <sup>28</sup>S. B. Palmer and E. W. Lee, *Philos. Mag.* **24**, 311 (1971).
- <sup>29</sup>K. W. Katahara, M. Nimalendran, M. H. Manghnani, and E. S. Fisher, *J. Phys. F* **9**, 2167 (1979).
- <sup>30</sup>E. E. Lähteenkorva and J. T. Lenkkeri, *J. Phys. F* **11**, 767 (1981).
- <sup>31</sup>W. C. Muir, J. M. Perz, and E. Fawcett, *J. Phys. F* **17**, 2431 (1987).
- <sup>32</sup>R. N. Thurston, *Proc. IEEE* **53**, 1320 (1965).
- <sup>33</sup>K. Brugger and T. C. Fritz, *Phys. Rev.* **157**, 524 (1967).
- <sup>34</sup>M. Cankurtaran, G. A. Saunders, Q. Wang, and H. L. Alberts (unpublished).
- <sup>35</sup>E. Fawcett, *J. Phys. Condens. Matter* **1**, 203 (1989).
- <sup>36</sup>E. Fawcett, A. B. Kaiser, and G. K. White, *Phys. Rev. B* **34**, 6248 (1986).
- <sup>37</sup>E. Fawcett, M. Acet, M. Shiga, and E. F. Wassermann, *Phys. Rev. B* **45**, 2180 (1992).
- <sup>38</sup>D. J. Kim, *Phys. Rev. B* **39**, 6844 (1989).
- <sup>39</sup>V. L. Moruzzi, *Phys. Rev. B* **41**, 6939 (1990).
- <sup>40</sup>Ll. Mañosa, G. A. Saunders, H. Rahdi, U. Kawald, J. Pelzl, and H. Bach, *J. Phys. Condens. Matter* **3**, 2273 (1991).
- <sup>41</sup>Ll. Mañosa, G. A. Saunders, H. Rahdi, U. Kawald, J. Pelzl, and H. Bach, *Phys. Rev. B* **45**, 2224 (1992).
- <sup>42</sup>M. Cankurtaran, G. A. Saunders, P. Ray, Q. Wang, U. Kawald, J. Pelzl, and H. Bach, *Phys. Rev. B* **47**, 3161 (1993).
- <sup>43</sup>G. A. Saunders, H. B. Senin, H. A. A. Sidek, and J. Pelzl, *Phys. Rev. B* **48**, 15 801 (1993).
- <sup>44</sup>K. Sumiyama, M. Shiga, M. Morioka, and Y. Nakamura, *J. Phys. F* **9**, 1665 (1979).
- <sup>45</sup>V. L. Moruzzi, *Physica B* **161**, 99 (1989).
- <sup>46</sup>V. L. Moruzzi, *Solid State Commun.* **83**, 739 (1992).
- <sup>47</sup>M. Shiga and Y. Nakamura, *J. Magn. Magn. Mater.* **90&91**, 733 (1990).
- <sup>48</sup>M. Shiga, Y. Kusakabe, Y. Nakamura, K. Makita, and M. Sogawa, *Physica B* **161**, 206 (1989).
- <sup>49</sup>V. A. Sidorov and L. G. Khvostantsev, *J. Magn. Magn. Mater.* **129**, 356 (1994).